Acta Crystallographica Section A
Foundations of Crystallography
ISSN 0108-7673

Received 10 October 2011
Accepted 11 December 2011

Covariance and correlation estimation in electron-density maps

Angela Altomare,[a] Corrado Cuocci,[a] Carmelo Giacovazzo,[a,b]* Anna Moliterni[a] and Rosanna Rizzi[a]

[a]Istituto di Cristallografia, Sede di Bari, Via G. Amendola 122/o, 70126 Bari, Italy, and [b]Dipartimento Geomineralogico, Università di Bari, Campus Universitario, Via Orabona 4, 70125 Bari, Italy. Correspondence e-mail: carmelo.giacovazzo@ic.cnr.it

Quite recently two papers have been published [Giacovazzo & Mazzone (2011). *Acta Cryst.* A**67**, 210–218; Giacovazzo *et al.* (2011). *Acta Cryst*. A**67**, 368–382] which calculate the variance in any point of an electron-density map at any stage of the phasing process. The main aim of the papers was to associate a standard deviation to each pixel of the map, in order to obtain a better estimate of the map reliability. This paper deals with the covariance estimate between points of an electron-density map in any space group, centrosymmetric or non-centrosymmetric, no matter the correlation between the model and target structures. The aim is as follows: to verify if the electron density in one point of the map is amplified or depressed as an effect of the electron density in one or more other points of the map. High values of the covariances are usually connected with undesired features of the map. The phases are the primitive random variables of our probabilistic model; the covariance changes with the quality of the model and therefore with the quality of the phases. The conclusive formulas show that the covariance is also influenced by the Patterson map. Uncertainty on measurements may influence the covariance, particularly in the final stages of the structure refinement; a general formula is obtained taking into account both phase and measurement uncertainty, valid at any stage of the crystal structure solution.

1. Notation

$F = \sum_{j=1}^{N} f_j \exp(2\pi i \mathbf{h}\cdot\mathbf{r}_j) = |F|\exp(i\varphi)$, structure factor of the target structure;
$F_p = \sum_{j=1}^{p} f_j \exp(2\pi i \mathbf{h}\cdot\mathbf{r}'_j) = |F_p|\exp(i\varphi_p)$, where $\mathbf{r}'_j = \mathbf{r}_j + \Delta\mathbf{r}_j$, structure factor of the model structure;
$\mathbf{C}_s \equiv (\mathbf{R}_s, \mathbf{T}_s)$, sth symmetry operator. $\mathbf{C}_s\,\mathbf{r} \equiv \mathbf{R}_s\mathbf{r} + \mathbf{T}_s$, where $\mathbf{R}_s$ and $\mathbf{T}_s$ are the rotational and translational matrices, respectively;
$\mathbf{C}_s^{-1}$, $\mathbf{R}_s^{-1}$, $\mathbf{T}_s^{-1}$, inverse matrices of $\mathbf{C}_s$, $\mathbf{R}_s$ and $\mathbf{T}_s$, respectively;
n, number of symmetry operators for the target and for the model structure;
$\sum_N = \sum_{j=1}^{N} f_j^2$;
$\sum_p = \sum_{j=1}^{p} f_j^2$;
$E = A + iB = R\exp(i\varphi)$, $E_p = A_p + iB_p = R_p\exp(i\varphi_p)$, $R = |F|/(\sum_N)^{1/2}$, $R_p = |F_p|/(\sum_p)^{1/2}$, normalized structure factors and their moduli;
$\rho(\mathbf{r}) = (2/V)\sum_{\mathbf{h}>0} |F_\mathbf{h}|\cos(2\pi\mathbf{h}\cdot\mathbf{r} - \varphi_\mathbf{h})$, general expression of an electron-density map;
$\rho_p(\mathbf{r}) = (2/V)\sum_{\mathbf{h}>0} |F_{p\mathbf{h}}|\cos(2\pi\mathbf{h}\cdot\mathbf{r} - \varphi_{p\mathbf{h}})$, electron-density map of the model structure;
$\rho_{\rm obs}(\mathbf{r}) = (2/V)\sum_{\mathbf{h}>0} m_\mathbf{h}|F_\mathbf{h}|\cos(2\pi\mathbf{h}\cdot\mathbf{r} - \varphi_{p\mathbf{h}})$, observed electron density when a model is available (m is defined below);
$P(\mathbf{u}) = (2/V)\sum_{\mathbf{h}>0} |F_\mathbf{h}|^2\cos(2\pi\mathbf{h}\cdot\mathbf{u})$, Patterson synthesis.

In all the above Fourier syntheses the term of order zero is omitted. Accordingly, the average values of the corresponding maps are always zero. By $\mathbf{h} > 0$ it is meant that the summation is over one half of reciprocal space (only one member of each Friedel pair is included).

$D_i(x) = I_i(x)/I_0(x)$, I_i is the modified Bessel function of order i;
$D = \langle\cos(2\pi\mathbf{h}\cdot\Delta\mathbf{r})\rangle$, the average is performed per resolution shell;
$\sigma_A = D(\Sigma_p/\Sigma_N)^{1/2}$;
$\sigma_R^2 = \langle|\mu|^2\rangle/\sum_N$, $\langle|\mu|^2\rangle^{1/2}$ is the expected value of the measurement error, usually assumed to coincide with its experimental standard deviation;
$e = 1 + \sigma_R^2$;
$m = \langle\cos(\varphi - \varphi_p)\rangle = I_1(X)/I_0(X)$, where $X = 2\sigma_A R R_p/(e - \sigma_A^2)$;
m is the weight to associate to each reflection in the non-centrosymmetric case. It coincides with the expected value of $\cos(\varphi - \varphi_p)$;
$m_c = \tanh(X/2)$, the weight to associate to each reflection in the centric case;
CORR, correlation between model and target electron-density maps.

2. Introduction

The study of the properties of electron-density maps started with W. H. Bragg in 1915 and continued with Bragg & West (1930), Booth (1946, 1947), Cruickshank (1949), Cochran (1951), and Cruickshank & Rollett (1953). Thanks to the above works, criteria were established for assessing the accuracy of the results of structure analysis. Among the other achievements, it was clearly established that truncation ripples displace peaks from their correct atomic positions, and that least squares are unbiased tools for the correct location of the atoms. Special attention was devoted to the effects of uncertainty of measurement; in particular Cruickshank (1949) calculated the expected mean square error in the electron density in the unit cell as

$$\sigma^2(\rho) = \frac{1}{V^2}\sum_{\mathbf{h}} \sigma^2(|F_{\mathbf{h}}|), \tag{1}$$

where $\sigma^2(|F_{\mathbf{h}}|)$ is the variance of the observed amplitude. A similar formula was obtained for the difference density $\Delta\rho = \rho_{\rm obs} - \rho_{\rm calc}$:

$$\sigma^2(\Delta\rho) = \frac{1}{V^2}\sum_{\mathbf{h}} \sigma^2(|F_{\mathbf{h}}|), \tag{2}$$

where $\rho_{\rm obs}$ and $\rho_{\rm calc}$ are the observed and the calculated electron densities. Data resolution was taken into account by replacing $\sigma^2(|F_{\mathbf{h}}|)$ with the expected value of $|F_{\mathbf{h}}|^2$ for all the reflections beyond the data termination.

The covariance in the deformation electron density was introduced by Rees (1976, 1978) to assess the meaningfulness of the structural model. The study concerned the function $\Delta\rho = \rho_{\rm obs}/k - \rho_{\rm c}$, where $\rho_{\rm obs}$ is the unscaled observed electron density eventually obtained after a multipolar refinement, k is the scale factor relating diffracted amplitudes and structure factors, and $\rho_{\rm c}$ is obtained from the refined model consisting of spherical atoms. The study took into account the errors in the experimental amplitudes, the errors on the model parameters and the errors in the scale factor.

In all the above works the emphasis was mainly focused on the errors connected to the mentioned parameters; indeed the final formulas find their applications in the last stages of crystal structure refinement, when the phases are considered well estimated and therefore are fixed parameters of the modelling.

Rees stated that covariance is useful if one wants to compare electron densities at two points in the same crystal (say $\mathbf{r}_A$ and $\mathbf{r}_B$), particularly when the chemical equivalence may be used to compute an average deformation electron density and therefore more precise information. Rees' investigation was limited to $P\overline{1}$, for which he obtained the following formula:

$$\langle\rho(\mathbf{r})\rho(\mathbf{r}+\mathbf{u})\rangle = \frac{2}{V^2}\sum_{\mathbf{h}>0}\sigma^2(|F_{\mathbf{h}}|)[\cos 2\pi\mathbf{h}\cdot(\mathbf{r}_A-\mathbf{r}_B) + \cos 2\pi\mathbf{h}\cdot(\mathbf{r}_A+\mathbf{r}_B)]. \tag{3}$$

Rees suggested that equation (3) may be extended to other centrosymmetric space groups by adding suitable symmetry elements (*e.g.* densities are calculated as for $P\overline{1}$ and then averaged over the symmetry-equivalent positions), but no general formula was derived.

We are interested in calculating the covariance between two points of an electron-density map in any space group, and to study its properties when a structural model is available, no matter whether it is of poor or of high quality. In this case the phases of the target structure cannot be considered as fixed parameters of the problem but as variables which determine the value of the covariance for any pair of points in the map. Under the above hypotheses the covariance expressions may be useful not only in the final stages of structure refinement but also during the phasing process.

We will use the same mathematical approach described by Giacovazzo & Mazzone (2011) for the $P1$ space group and by Giacovazzo *et al.* (2011) for any centrosymmetric and non-centrosymmetric space group. In particular we will assume that each target phase $\varphi_{\mathbf{h}}$ is distributed around the model phase $\varphi_{p\mathbf{h}}$ according to the von Mises distribution (von Mises, 1918),

$$M(\varphi; X, \varphi_p) = [2\pi I_0(X)]^{-1}\exp[X\cos(\varphi-\varphi_p)]. \tag{4}$$

Under this hypothesis we are able to estimate the covariance no matter the correlation between the model and target structures. In particular, when CORR = 0 equation (4) is equivalent to a random distribution; when CORR $\sim$1 the phase distribution coincides with the Dirac delta function.

In the first part of this paper we will study a basic component of the covariance, say the joint moment $\langle\rho(\mathbf{r})\rho(\mathbf{r}+\mathbf{u})\rangle$, first in $P1$ and then in all centrosymmetric and non-centrosymmetric space groups. In §§7–8 the covariance expression is derived for any type of hybrid electron-density map, in §9 the correlation formula is obtained, and in §10 a general expression of the covariance taking into account both phase and measurement uncertainty is given.

Some few additional comments are necessary to better describe the aim, the limits and the potential of this paper:

(i) A crystal structure solution process usually ends with a set of atomic parameters; they are published together with corresponding standard deviations, which act as accuracy criteria. Least squares are considered a fundamental tool in crystallography just because they provide optimal values for the parameters, for their variances and covariances; they are usually inefficient if covariance between parameters is high.

(ii) It is not usual in crystallography to associate the variance to an electron-density map, even if it is the standard deviation, calculated at each pixel of the map, which states how reliable is the density value at that pixel. This practice is unsatisfactory because in all the cases in which a parameter is part of a model, the associated variance should be calculated. The practice for the electron densities was certainly originated by a lack of theory, only recently supplied by Giacovazzo & Mazzone (2011) and Giacovazzo *et al.* (2011), who provided a tool for estimating the quality of an electron-density map in each point $\mathbf{r}$ of the map at any stage of the phasing process, no matter if an observed, a difference or a hybrid electron density

was calculated. The practice, however, was also facilitated by the fact that least-squares cycles, which often follow the electron-density map analysis, are an efficient succedaneum: indeed they provide the required standard deviations for the structural parameters, and calculate covariance between them.

(iii) Covariance, or correlation, between two points of an electron-density map is a signal for understanding if the electron density in one point of the map is amplified or depressed as an effect of the electron density in another point of the map. Electron-density maps are strongly affected by covariance effects; ripples associated with peaks are a typical example, but also pseudotranslational symmetry is a frequent source of covariance. This paper establishes the mathematical formulas for calculating covariances between peak densities at any step of the phasing process (in some way, it is the counterpart in real space of least-squares covariance calculations). As we will see in this paper, large covariances indicate undesired features of the map.

(iv) Covariance itself is not a new tool for solving crystal structures. The approach described in this paper does not aim to correct the standard deviation of the experimental intensities or the intensities themselves; it only uses the experimental values and the current phases for calculating covariances in an electron-density map. Inevitably errors in the experimental values or in the phases will lead to errors in covariances. In spite of this limitation, the theory described in this paper has inspired a new technique for solving crystal structures from powder data (Altomare *et al.*, to be submitted).

(v) For calculating covariance maps for practical cases fast Fourier transform (FFT) is mandatory. This is the reason why in this paper the main covariance features have been studied in simple one-dimensional cases. In a paper in preparation (Giacovazzo & Mazzone, to be submitted) it is shown how FFT may be used for calculating variance maps; we hope to extend the method for calculating covariances.

3. About the joint moment $\langle\rho(\mathbf{r})\rho(\mathbf{r}+\mathbf{u})\rangle$ in *P*1

We will calculate the joint moment

$$\langle\rho(\mathbf{r})\rho(\mathbf{r}+\mathbf{u})\rangle = \frac{4}{V^2}\left\langle \sum_{\mathbf{h},\mathbf{k}>0} \left|F_{\mathbf{h}}F_{\mathbf{k}}\right| \cos(2\pi\mathbf{h}\cdot\mathbf{r}-\varphi_{\mathbf{h}}) \times \cos[2\pi\mathbf{k}\cdot(\mathbf{r}+\mathbf{u})-\varphi_{\mathbf{k}}]\right\rangle \quad (5)$$

under the assumption of equation (4). This assumption is quite common in phasing procedures; at a certain stage of the phasing process a model becomes available, from which the reliability factor $X_{\mathbf{h}}$ may be calculated for each reflection (Sim, 1959; Srinivasan & Ramachandran, 1965; Read, 1986; Burla *et al.*, 2011).

Under the hypothesis of equation (4) and by assuming that phases $\varphi_{\mathbf{h}}$ and $\varphi_{\mathbf{k}}$ are statistically independent of each other, equation (5) reduces to

$$\begin{aligned}\langle\rho(\mathbf{r})\rho(\mathbf{r}+\mathbf{u})\rangle = {} & \frac{2}{V^2}\sum_{\mathbf{h}>0}\left|F_{\mathbf{h}}\right|^2\cos 2\pi\mathbf{h}\cdot\mathbf{u} + \frac{2}{V^2}\sum_{\mathbf{h}>0}\left|F_{\mathbf{h}}\right|^2 D_2(X_{\mathbf{h}}) \\ & \times\cos(2\pi\mathbf{h}\cdot\mathbf{u}+4\pi\mathbf{h}\cdot\mathbf{r}-2\varphi_{p\mathbf{h}}) \\ & + \frac{4}{V^2}\sum_{\mathbf{h}\neq\mathbf{k}>0}\left|F_{\mathbf{h}}F_{\mathbf{k}}\right| m_{\mathbf{h}}m_{\mathbf{k}}\cos(2\pi\mathbf{h}\cdot\mathbf{r}-\varphi_{p\mathbf{h}}) \\ & \times\cos[2\pi\mathbf{k}\cdot(\mathbf{r}+\mathbf{u})-\varphi_{p\mathbf{k}}]. \end{aligned} \quad (6)$$

We notice now that

$$\begin{aligned}\rho_{\rm obs}(\mathbf{r})\rho_{\rm obs}(\mathbf{r}+\mathbf{u}) = {} & \frac{4}{V^2}\sum_{\mathbf{h}>0}\left|F_{\mathbf{h}}\right|^2 m_{\mathbf{h}}^2\cos(2\pi\mathbf{h}\cdot\mathbf{r}-\varphi_{p\mathbf{h}}) \\ & \times\cos[2\pi\mathbf{h}\cdot(\mathbf{r}+\mathbf{u})-\varphi_{p\mathbf{h}}] \\ & + \frac{4}{V^2}\sum_{\mathbf{h}\neq\mathbf{k}>0}\left|F_{\mathbf{h}}F_{\mathbf{k}}\right| m_{\mathbf{h}}m_{\mathbf{k}}\cos(2\pi\mathbf{h}\cdot\mathbf{r}-\varphi_{p\mathbf{h}}) \\ & \times\cos[2\pi\mathbf{k}\cdot(\mathbf{r}+\mathbf{u})-\varphi_{p\mathbf{k}}], \end{aligned} \quad (7)$$

and therefore the last term of equation (6) may be estimated *via* equation (7). Finally we obtain

$$\langle\rho(\mathbf{r})\rho(\mathbf{r}+\mathbf{u})\rangle = T_{\rm obs} + T_1 + T_2, \quad (8)$$

where

$$\begin{aligned} T_{\rm obs}(\mathbf{r},\mathbf{r}+\mathbf{u}) &= \rho_{\rm obs}(\mathbf{r})\rho_{\rm obs}(\mathbf{r}+\mathbf{u}), \\ T_1(\mathbf{r},\mathbf{r}+\mathbf{u}) &= \frac{2}{V^2}\sum_{\mathbf{h}>0}\left|F_{\mathbf{h}}\right|^2(1-m_{\mathbf{h}}^2)\cos 2\pi\mathbf{h}\cdot\mathbf{u}, \\ T_2(\mathbf{r},\mathbf{r}+\mathbf{u}) &= -\frac{2}{V^2}\sum_{\mathbf{h}>0}\left|F_{\mathbf{h}}\right|^2[m_{\mathbf{h}}^2 - D_2(X_{\mathbf{h}})] \\ &\quad\times\cos(4\pi\mathbf{h}\cdot\mathbf{r}+2\pi\mathbf{h}\cdot\mathbf{u}-2\varphi_{p\mathbf{h}}). \end{aligned}$$

We observe:

(*a*) Given the prior knowledge of the model structure $\rho_p(\mathbf{r})$ (and therefore of the phases $\varphi_{p\mathbf{h}}$) the joint moment $\langle\rho(\mathbf{r})\rho(\mathbf{r}+\mathbf{u})\rangle$ may be represented by a six-dimensional map. Indeed for each point $\mathbf{r}_A$ a three-dimensional map $\langle\rho(\mathbf{r}_A)\rho(\mathbf{r}_A+\mathbf{u})\rangle$ may be drawn. Equation (8) suggests that the joint moment is not a decreasing function of the distance $|\mathbf{u}|$.

(*b*) $\langle\rho(\mathbf{r})\rho(\mathbf{r}+\mathbf{u})\rangle$ is the sum of three terms.

$T_{\rm obs}$ is a non-centrosymmetric function, phase and therefore model dependent. In particular it coincides with the product of the observed electron densities in $\mathbf{r}$ and $\mathbf{r}+\mathbf{u}$: it vanishes if $\rho_{\rm obs}(\mathbf{r})$ and/or $\rho_{\rm obs}(\mathbf{r}+\mathbf{u})$ vanish. The largest joint moment values will probably concern pairs of points $(\mathbf{r},\mathbf{r}+\mathbf{u})$ where the observed electron density is large.

T_1 is a centrosymmetrical function of $\mathbf{u}$; it is a weighted Patterson function which may be described as a difference of Patterson maps:

$$T_1 = V^{-1}[P(\mathbf{u}) - P_{\rm w}(\mathbf{u})],$$

where $P_{\rm w}(\mathbf{u})$ is the map calculated *via* coefficients $m_{\mathbf{h}}^2|F_{\mathbf{h}}|^2$. If CORR = 0, then $T_1 = V^{-1}P(\mathbf{u})$; if CORR = 1 then T_1 vanishes.

If CORR is far from zero and 1, the weights minimize the contribution of the reflections with the largest observed and calculated amplitudes (for which $m_{\mathbf{h}}^2 \approx 1$). In this case T_1 contributes to the joint moment $\langle\rho(\mathbf{r})\rho(\mathbf{r}+\mathbf{u})\rangle$ mostly through reflections with large observed and small calculated values.

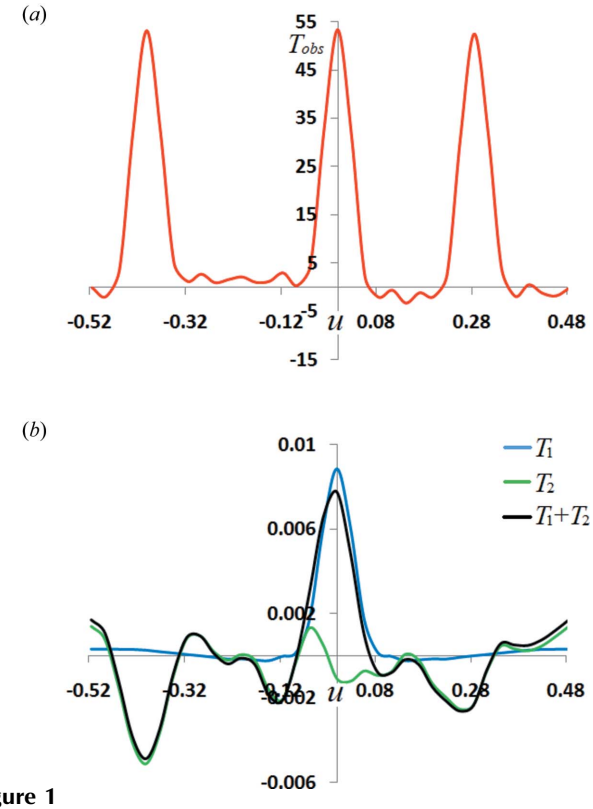

Figure 1
Case 1: model and target structures nearly coincident (0.91 Å resolution data). Components of the $\langle\rho(z_{O3})\rho(z_{O3}+u)\rangle$ moment: (*a*) T_{obs} *versus* u; (*b*) T_1 and T_2 *versus* u (in blue and green, respectively). The covariance (T_1 + T_2) is drawn in black.

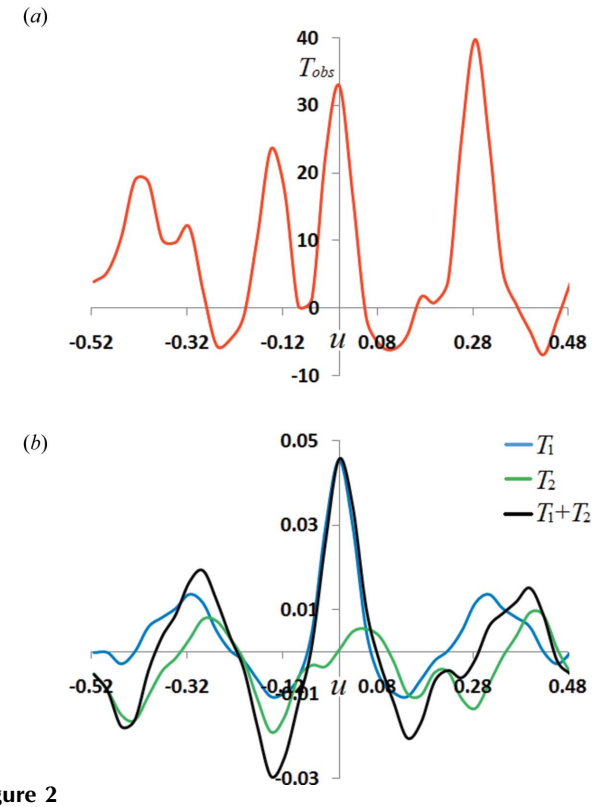

Figure 2
Case 2: target structure as in Fig. 1, model structure as in Fig. 1 but O1 was moved from the original position (0.91 Å resolution data). Components of the $\langle\rho(z_{O3})(z_{O3}+u)\rangle$ moment: (*a*) T_{obs} *versus* u; (*b*) T_1 and T_2 *versus* u (in blue and green, respectively). The covariance (T_1 + T_2) is drawn in black.

T_2 is a six-dimensional weighted Fourier synthesis, a function of **r** and **u**, belonging to a special category of 'observed syntheses', denoted FF synthesis by Burla *et al.* (2006) and by Caliandro *et al.* (2007). It uses $|F|^2$ observed moduli as the standard Patterson function, but it combines them with calculated phases $2\varphi_{p\mathbf{h}}$ [*e.g.* the typical coefficient of a Patterson function is $F_{\mathbf{h}}F_{-\mathbf{h}} = |F_{\mathbf{h}}|^2$, that of the FF synthesis is $F_{\mathbf{h}}F_{\mathbf{h}} = |F_{\mathbf{h}}|^2 \exp(i2\varphi_{p\mathbf{h}})$]. The FF synthesis is expected to show maxima at $\mathbf{r}_i + \mathbf{r}_j$ (they will correspond to negative minima of T_2), where $\mathbf{r}_i$ and $\mathbf{r}_j$ are atomic positional vectors. The weight $m_{\mathbf{h}}^2 - D_2(X_{\mathbf{h}})$ of T_2 is always non-negative, is everywhere smaller than $(1 - m_{\mathbf{h}}^2)$ and its value vanishes at $X = 0$ and $X = \infty$.

T_2 is a non-centrosymmetric function: for a given vector **u** it shows a three-dimensional periodicity in **r**, half that of the electron density. Indeed it assumes the same value in **r** and in $\mathbf{r} + \Delta\mathbf{r}$, where $\Delta\mathbf{r} = \Delta x\mathbf{a} + \Delta y\mathbf{b} + \Delta z\mathbf{c}$. Δx, Δy, Δz may independently assume the values 0 or 1/2.

(*c*) If the model is uncorrelated with the target structure, T_{obs} vanishes (because $m_{\mathbf{h}}$ vanishes for all reflections), T_1 coincides with the Patterson synthesis and T_2 vanishes too. In short

$$\langle\rho(\mathbf{r})\rho(\mathbf{r}+\mathbf{u})\rangle_{\rm uncorr} = V^{-1}P(\mathbf{u}). \qquad (9)$$

Equation (9) reminds us that, in the absence of phase information, for a given random model, $\langle\rho(\mathbf{r})\rho(\mathbf{r}+\mathbf{u})\rangle_{\rm uncorr}$ may still be different from zero provided the Patterson map is not vanishing in **u**. To give a simple idea of the practical consequences, let us choose in the $\rho_{\rm obs}$ map a generic peak defined by the positional vector $\mathbf{r}_A$. Even if CORR = 0, the pixel of the $\rho_{\rm obs}$ map located at $\mathbf{r}_B = \mathbf{r} + \mathbf{u}$ is expected to have (but not necessarily has) a non-vanishing density provided the Patterson map shows a peak in **u**. Such a result is not surprising; indeed the Patterson function is independent of the phases, and just suggests that the value of the joint moment $\langle\rho(\mathbf{r})\rho(\mathbf{r}+\mathbf{u})\rangle$ is not vanishing if $P(\mathbf{u})$ shows a peak in **u**.

(*d*) If CORR ∼1, then the phases are no more free variables and their distributions coincide with Dirac delta functions. In this case T_1 and T_2 vanish, and

$$\langle\rho(\mathbf{r})\rho(\mathbf{r}+\mathbf{u})\rangle_{\rm corr} = \rho_{\rm obs}(\mathbf{r})\rho_{\rm obs}(\mathbf{r}+\mathbf{u}).$$

(*e*) In non-extreme cases (*e.g.* when a model is available with correlation far away from 0 or 1), the joint moment $\langle\rho(\mathbf{r})\rho(\mathbf{r}+\mathbf{u})\rangle$ is the sum of three contributions. All of them concur to establish the value of the joint moment, with constructive or destructive interference. It may be useful to check if, in some conditions, one of $T_{\rm obs}$, T_1 or T_2 is negligible with respect to the others. We consider as an example an (unrealistic) *P*1 structure (the target structure) with $a = 5.45$, $b = 6.56$, $c = 12.11$ Å, $\alpha = 106$, $\beta = 96$, $\gamma = 78^\circ$.

The three O atoms constituting the structure were all located along the *c* axis, at $z_{O1} = 0.114$, $z_{O2} = 0.800$, $z_{O3} = 0.514$,

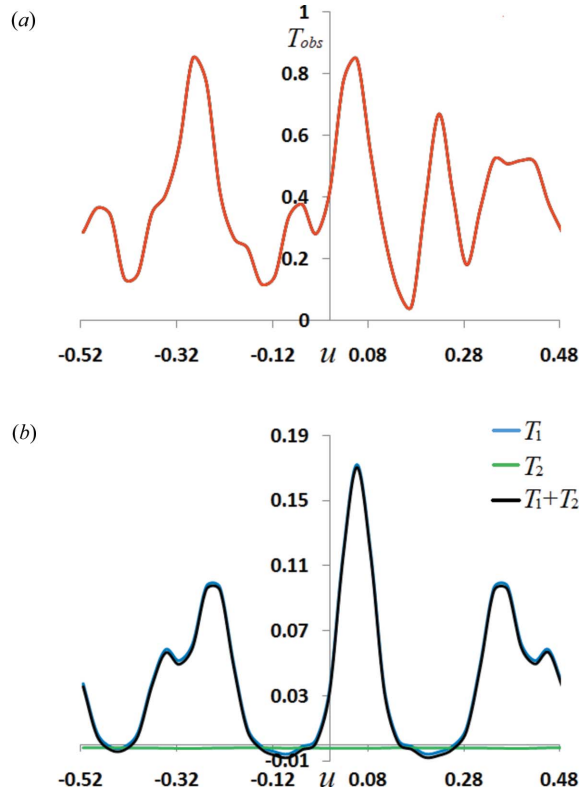

Figure 3
Case 3: target structure as in Fig. 1, the three O atoms of the model structure moved far away from the original positions (0.91 Å resolution data). Components of the $\langle\rho(z_{O3})(z_{O3}+u)\rangle$ moment: (*a*) T_{obs} *versus* u; (*b*) T_1 and T_2 *versus* u (in blue and green, respectively). The covariance (T_1 + T_2) is drawn in black.

to easily depict in one dimension the joint moment components. We want to estimate $\langle\rho(z_{O3})\rho(z_{O3}+u)\rangle$ *versus* u; in other words, we will calculate the joint moment with respect to the O3 peak as a function of the distance u from the O3 position. The three terms on the right-hand side of equation (8) have been calculated and plotted in Figs. 1–3 for three structure models (data up to 0.91 Å resolution). In each figure the red, blue and green lines represent T_{obs}, T_1 and T_2, respectively.

Case 1 (see Fig. 1). The model nearly coincides with the target. We calculated for $\langle\sigma_A\rangle$ (*i.e.* the average of the σ_A values computed per resolution shell) the value of 0.95: $m_{\mathbf{h}}$ is close to unity for all the largest reflections. The joint moment $\langle\rho(z_{O3})\rho(z_{O3}+u)\rangle$ practically coincides with T_{obs}, as theoretically expected. Three T_{obs} peaks are visible in Fig. 1(*a*), corresponding to the distances O1—O3, O3—O3 and O2—O3. T_1 and T_2 are negligible with respect to T_{obs} (see Fig. 1*b*). T_1 shows an origin peak, as expected for a Patterson-like function, much smaller than T_{obs} peaks.

T_2 is expected to show negative peaks at the positions $z_{O1}+z_{O2}=-0.09$, $z_{O1}+z_{O3}=-0.37$, $z_{O2}+z_{O3}=0.31$ which are visible in Fig. 1(*b*) (the last one a bit shifted).

Case 2 (see Fig. 2). We moved O1 to $z_{O1}=0.37$, the other two atoms remain in their original positions. The model is well correlated with the target ($\langle\sigma_A\rangle=0.75$) and $m_{\mathbf{h}}$ is close to unity for the largest observed reflections. T_{obs} is still dominant: peaks corresponding to the distances O1—O3 and O2—O3 in both the target and model structures can be recognized (this information is usually present in the observed electron densities). T_1 shows a main peak at the origin, as expected for Patterson-like functions, as well as faint peaks in correspondence of the target distances O2—O3 and O1—O3. T_2 negative peaks are in correspondence with the $\mathbf{r}_i+\mathbf{r}_j$ positions as present in both model and target structures (in accordance with the observed nature of the FF synthesis).

Case 3 (see Fig. 3). We moved the three atoms to new positions, say $z_{O1}=0.23$, $z_{O2}=0.74$, $z_{O3}=0.57$. The model is practically uncorrelated with the target: we calculated $\sigma_A=0.1$. T_{obs} is still dominant with respect to T_1 and T_2 (it may be neglected only at σ_A values very close to zero); its average intensity is strongly diminished with respect to cases 1 and 2. T_2 is vanishing and flat everywhere, T_1 shows a main peak at the origin (much smaller than the main peak of T_{obs}), and two wide peaks mostly including the target interatomic distances.

(*f*) $\langle\rho(\mathbf{r})\rho(\mathbf{r}+\mathbf{u})\rangle$ depends on the data resolution: the better the resolution, the larger the number of structure-factor moduli contributing to the summations in equation (8).

We rewrite equation (8) in a notation (say $\mathbf{r}=\mathbf{r}_A$ and $\mathbf{u}=\mathbf{r}_B-\mathbf{r}_A$) which will allow us a more direct comparison with the formula [see equation (3)] obtained by Rees in $P\overline{1}$. We obtain

$$\begin{aligned}\langle\rho(\mathbf{r}_A)\rho(\mathbf{r}_B)\rangle &= \rho_{obs}(\mathbf{r}_A)\rho_{obs}(\mathbf{r}_B)+\frac{2}{V^2}\sum_{\mathbf{h}>0}|F_{\mathbf{h}}|^2(1-m_{\mathbf{h}}^2)\\ &\times\cos[2\pi\mathbf{h}\cdot(\mathbf{r}_A-\mathbf{r}_B)]\\ &-\frac{2}{V^2}\sum_{\mathbf{h}>0}|F_{\mathbf{h}}|^2[m_{\mathbf{h}}^2-D_2(X_{\mathbf{h}})]\\ &\times\cos[2\pi\mathbf{h}\cdot(\mathbf{r}_A+\mathbf{r}_B)-2\varphi_{p\mathbf{h}}].\end{aligned}\tag{10}$$

4. The estimate of the joint moment $\langle\rho(\mathbf{r})\rho(\mathbf{r}+\mathbf{u})\rangle$ in $P\overline{1}$

The $\rho(\mathbf{r})$ expression for $P\overline{1}$ does not substantially change with respect to that used for $P1$; the only difference is that φ may only assume the values 0 or π. In our calculations we will assume that φ_p may only get the values 0 or π, that $\varphi=\varphi_p$ or $\varphi=\varphi_p+\pi$ according to circumstances, and that the weight m_c may be associated with the relation $\varphi\approx\varphi_p$. Then

$$\langle\rho(\mathbf{r})\rangle=\frac{2}{V}\sum_{\mathbf{h}>0}m_{c\mathbf{h}}|F_{\mathbf{h}}|\cos(2\pi\mathbf{h}\cdot\mathbf{r}-\varphi_{p\mathbf{h}})=\rho_{obs}(\mathbf{r}).$$

After some calculations, similar to those described in §3, we obtain

$$\begin{aligned}\langle\rho(\mathbf{r}_A)\rho(\mathbf{r}_B)\rangle &= \rho_{obs}(\mathbf{r}_A)\rho_{obs}(\mathbf{r}_B)+\frac{2}{V^2}\sum_{\mathbf{h}>0}|F_{\mathbf{h}}|^2(1-m_{c\mathbf{h}}^2)\\ &\times\{\cos[2\pi\mathbf{h}\cdot(\mathbf{r}_A-\mathbf{r}_B)]+\cos[2\pi\mathbf{h}\cdot(\mathbf{r}_A+\mathbf{r}_B)]\}.\end{aligned}\tag{11}$$

We notice:

(i) In $P\bar{1}$ both $\mathbf{r}_A - \mathbf{r}_B$ and $\mathbf{r}_A + \mathbf{r}_B$ are interatomic vectors; therefore

$$\begin{aligned}\langle\rho(\mathbf{r}_A)\rho(\mathbf{r}_B)\rangle &= \rho_{\rm obs}(\mathbf{r}_A)\rho_{\rm obs}(\mathbf{r}_B)\\ &+ V^{-1}[P(\mathbf{r}_A - \mathbf{r}_B) - P_{wc}(\mathbf{r}_A - \mathbf{r}_B)]\\ &+ V^{-1}[P(\mathbf{r}_A + \mathbf{r}_B) - P_{wc}(\mathbf{r}_A + \mathbf{r}_B)], \quad (12)\end{aligned}$$

where P_{wc} is the Patterson function calculated with coefficients $m_{c\mathbf{h}}^2|F_{\mathbf{h}}|^2$.

Equation (12) takes full account of the symmetry. Indeed, when $\mathbf{r}_B = \mathbf{r}_A$ or $\mathbf{r}_B = -\mathbf{r}_A$ (in this last case $\mathbf{r}_B$ and $\mathbf{r}_A$ are symmetry-equivalent positions) we have

$$\begin{aligned}\langle\rho(\mathbf{r}_A)\rho(\mathbf{r}_B)\rangle = \langle\rho^2(\mathbf{r}_A)\rangle &= \rho_{\rm obs}^2(\mathbf{r}_A) + V^{-1}[P(0) - P_{wc}(0)]\\ &+ V^{-1}[P(2\mathbf{r}_A) - P_{wc}(2\mathbf{r}_A)]. \quad (13)\end{aligned}$$

(ii) If the model is uncorrelated with the target structure, then $\rho_{\rm obs}(\mathbf{r}_A)\rho_{\rm obs}(\mathbf{r}_B) = 0$ and

$$\langle\rho(\mathbf{r}_A)\rho(\mathbf{r}_B)\rangle = \frac{1}{V}[P(\mathbf{r}_A - \mathbf{r}_B) + P(\mathbf{r}_A + \mathbf{r}_B)].$$

If, in addition, $\mathbf{r}_B = \mathbf{r}_A$ or $\mathbf{r}_B = -\mathbf{r}_A$ then

$$\langle\rho^2(\mathbf{r}_A)\rangle = V^{-1}[P(0) + P(2\mathbf{r}_A)].$$

(iii) If the model is highly correlated with the target, the joint moment is totally dominated by $T_{\rm obs}$. Situations in between cases (ii) and (iii) can be easily understood on the basis of the above considerations and of those described in §3.

5. About the joint moment $\langle\rho(\mathbf{r})\rho(\mathbf{r}+\mathbf{u})\rangle$ in any non-centrosymmetric space group

Owing to the well known symmetry relationship

$$F_{\mathbf{hR}} = F_{\mathbf{h}}\exp(-2\pi i\mathbf{hT}) = |F_{\mathbf{h}}|\exp[i(\varphi_{\mathbf{h}} - 2\pi\mathbf{hT})],$$

the general expression of the electron density for an acentric space group is

$$\rho(\mathbf{r}) = \frac{2}{V}\sum_{\mathbf{h},\rm ind}|F_{\mathbf{h}}|\sum_{s=1}^{n}\cos[\varphi(\mathbf{h}) - 2\pi\mathbf{hC}_s\mathbf{r}].$$

If each phase $\varphi_{\mathbf{h}}$ is assumed to be distributed around $\varphi_{p\mathbf{h}}$ according to the von Mises distribution [equation (4)], then

$$\begin{aligned}\langle\rho(\mathbf{r})\rho(\mathbf{r}+\mathbf{u})\rangle = \frac{2}{V^2}\sum_{\mathbf{h},\rm ind}|F_{\mathbf{h}}|^2 D_2(X_{\mathbf{h}})\sum_{s,q=1}^{n}\cos\{2\varphi_p(\mathbf{h})\\ - 2\pi\mathbf{h}[\mathbf{C}_s\mathbf{r} + \mathbf{C}_q(\mathbf{r}+\mathbf{u})]\}\\ + \frac{2}{V^2}\sum_{\mathbf{h},\rm ind}|F_{\mathbf{h}}|^2\sum_{s,q=1}^{n}\cos 2\pi\mathbf{h}[\mathbf{C}_s\mathbf{r} - \mathbf{C}_q(\mathbf{r}+\mathbf{u})]\\ + \frac{4}{V^2}\sum_{\mathbf{h}\neq\mathbf{k},\rm ind} m_{\mathbf{h}}m_{\mathbf{k}}|F_{\mathbf{h}}F_{\mathbf{k}}|\sum_{s,q=1}^{n}\cos[\varphi_p(\mathbf{h})\\ - 2\pi\mathbf{hC}_s\mathbf{r}]\cos[\varphi_p(\mathbf{k}) - 2\pi\mathbf{kC}_q(\mathbf{r}+\mathbf{u})].\end{aligned}$$

Since

$$\begin{aligned}\rho_{\rm obs}(\mathbf{r})\rho_{\rm obs}(\mathbf{r}+\mathbf{u}) = \frac{2}{V^2}\sum_{\mathbf{h},\rm ind} m_{\mathbf{h}}^2|F_{\mathbf{h}}|^2\Bigg(\sum_{s,q=1}^{n}\cos\{2\varphi_p(\mathbf{h})\\ - 2\pi\mathbf{h}[\mathbf{C}_s\mathbf{r} + \mathbf{C}_q(\mathbf{r}+\mathbf{u})]\}\\ + \sum_{s,q=1}^{n}\cos 2\pi\mathbf{h}[\mathbf{C}_s\mathbf{r} - \mathbf{C}_q(\mathbf{r}+\mathbf{u})]\Bigg)\\ + \frac{4}{V^2}\sum_{\mathbf{h}\neq\mathbf{k},\rm ind} m_{\mathbf{h}}m_{\mathbf{k}}|F_{\mathbf{h}}F_{\mathbf{k}}|\sum_{s,q=1}^{n}\cos[\varphi_p(\mathbf{h})\\ - 2\pi\mathbf{hC}_s\mathbf{r}]\cos[\varphi_p(\mathbf{k}) - 2\pi\mathbf{kC}_q(\mathbf{r}+\mathbf{u})],\end{aligned}$$

then

$$\begin{aligned}\langle\rho(\mathbf{r})\rho(\mathbf{r}+\mathbf{u})\rangle = \rho_{\rm obs}(\mathbf{r})\rho_{\rm obs}(\mathbf{r}+\mathbf{u}) + 2V^{-2}\sum_{\mathbf{h},\rm ind}|F_{\mathbf{h}}|^2(1-m_{\mathbf{h}}^2)\\ \times\sum_{s,q=1}^{n}\cos 2\pi\mathbf{h}[\mathbf{C}_s\mathbf{r} - \mathbf{C}_q(\mathbf{r}+\mathbf{u})]\\ - 2V^{-2}\sum_{\mathbf{h},\rm ind}|F_{\mathbf{h}}|^2[m_{\mathbf{h}}^2 - D_2(X_{\mathbf{h}})]\\ \times\sum_{s,q=1}^{n}\cos\{2\varphi_p(\mathbf{h}) - 2\pi\mathbf{h}[\mathbf{C}_s\mathbf{r} + \mathbf{C}_q(\mathbf{r}+\mathbf{u})]\}.\end{aligned}$$

If we use the notation $\mathbf{r} = \mathbf{r}_A$ and $\mathbf{u} = \mathbf{r}_B - \mathbf{r}_A$ we have

$$\langle\rho(\mathbf{r}_A)\rho(\mathbf{r}_B)\rangle = T_{\rm obs} + T_{1a} + T_{2a}, \quad (14)$$

where

$$\begin{aligned}T_{\rm obs}(\mathbf{r}_A,\mathbf{r}_B) &= \rho_{\rm obs}(\mathbf{r}_A)\rho_{\rm obs}(\mathbf{r}_B),\\ T_{1a}(\mathbf{r}_A,\mathbf{r}_B) &= 2V^{-2}\sum_{\mathbf{h},\rm ind}|F_{\mathbf{h}}|^2(1-m_{\mathbf{h}}^2)\\ &\times\sum_{s,q=1}^{n}\cos[2\pi\mathbf{h}(\mathbf{C}_s\mathbf{r}_A - \mathbf{C}_q\mathbf{r}_B)], \quad (15a)\end{aligned}$$

$$\begin{aligned}T_{2a}(\mathbf{r}_A,\mathbf{r}_B) = -2V^{-2}\sum_{\mathbf{h},\rm ind}|F_{\mathbf{h}}|^2[m_{\mathbf{h}}^2 - D_2(X_{\mathbf{h}})]\\ \times\sum_{s,q=1}^{n}\cos[2\varphi_p(\mathbf{h}) - 2\pi\mathbf{h}(\mathbf{C}_s\mathbf{r}_A + \mathbf{C}_q\mathbf{r}_B)]. \quad (15b)\end{aligned}$$

It may be worthwhile noticing that the term

$$2V^{-2}\sum_{\mathbf{h},\rm ind}|F_{\mathbf{h}}|^2(1-m_{\mathbf{h}}^2)\sum_{s=1}^{n}\cos[2\pi\mathbf{hC}_s(\mathbf{r}_A - \mathbf{r}_B)]$$

is part of $T_{1a}(\mathbf{r}_A,\mathbf{r}_B)$, obtained when $s = q$.

T_{1a} and T_{2a} may be rewritten (see Appendix A) in the form

$$T_{1a}(\mathbf{r}_A,\mathbf{r}_B) = \frac{2}{V^2}\sum_{\mathbf{h}>0}|F_{\mathbf{h}}|^2(1-m_{\mathbf{h}}^2)\sum_{s=1}^{n}\cos[2\pi\mathbf{h}(\mathbf{r}_A - \mathbf{C}_s\mathbf{r}_B)] \quad (16a)$$

$$\begin{aligned}T_{2a}(\mathbf{r}_A,\mathbf{r}_B) = -\frac{2}{V^2}\sum_{\mathbf{h}>0}|F_{\mathbf{h}}|^2[m_{\mathbf{h}}^2 - D_2(X_{\mathbf{h}})]\\ \times\sum_{s=1}^{n}\cos[2\varphi_p(\mathbf{h}) - 2\pi\mathbf{h}(\mathbf{r}_A + \mathbf{C}_s\mathbf{r}_B)]. \quad (16b)\end{aligned}$$

6. About the joint moment $\langle\rho(\mathbf{r})\rho(\mathbf{r}+\mathbf{u})\rangle$ in any centrosymmetric space group

In a centric space group of order n the electron density may be expressed as

$$\rho(\mathbf{r}) = 2V^{-1}\sum_{\mathbf{h},\mathrm{ind}}|F_{\mathbf{h}}|\sum_{s=1}^{n/2}\cos[\varphi(\mathbf{h}) - 2\pi\mathbf{h}\mathbf{C}_s\mathbf{r}],$$

where $n/2$ is the number of symmetry operators not referred by an inversion centre (see Giacovazzo *et al.*, 2011). Accordingly

$$\langle\rho(\mathbf{r})\rangle = 2V^{-1}\sum_{\mathbf{h},\mathrm{ind}} m_{c\mathbf{h}}|F_{\mathbf{h}}|\sum_{s=1}^{n/2}\cos[\varphi_p(\mathbf{h}) - 2\pi\mathbf{h}\mathbf{C}_s\mathbf{r}] = \rho_{\mathrm{obs}}(\mathbf{r}).$$

The application of the same mathematical procedure described in §5 leads to

$$\begin{aligned}\langle\rho(\mathbf{r})\rho(\mathbf{r}+\mathbf{u})\rangle &= 2V^{-2}\sum_{\mathbf{h},\mathrm{ind}}\left|F_{\mathbf{h}}\right|^2\sum_{s,q=1}^{n/2}\cos 2\pi\mathbf{h}[\mathbf{C}_s\mathbf{r} + \mathbf{C}_q(\mathbf{r}+\mathbf{u})]\\ &+ 2V^{-2}\sum_{\mathbf{h},\mathrm{ind}}\left|F_{\mathbf{h}}\right|^2\sum_{s,q=1}^{n/2}\cos 2\pi\mathbf{h}[\mathbf{C}_s\mathbf{r} - \mathbf{C}_q(\mathbf{r}+\mathbf{u})]\\ &+ 4V^{-2}\sum_{\mathbf{h}\neq\mathbf{k},\mathrm{ind}} m_{c\mathbf{h}}m_{c\mathbf{k}}|F_{\mathbf{h}}F_{\mathbf{k}}|\sum_{s,q=1}^{n/2}\cos[\varphi_p(\mathbf{h})\\ &- 2\pi\mathbf{h}\mathbf{C}_s\mathbf{r}]\cos[\varphi_p(\mathbf{k}) - 2\pi\mathbf{k}\mathbf{C}_q(\mathbf{r}+\mathbf{u})].\end{aligned}$$

Since

$$\begin{aligned}\rho_{\mathrm{obs}}(\mathbf{r})\rho_{\mathrm{obs}}(\mathbf{r}+\mathbf{u}) &= 2V^{-2}\sum_{\mathbf{h},\mathrm{ind}} m_{c\mathbf{h}}^2\left|F_{\mathbf{h}}\right|^2\Bigg\{\sum_{s,q=1}^{n/2}\cos 2\pi\mathbf{h}[\mathbf{C}_s\mathbf{r}\\ &+ \mathbf{C}_q(\mathbf{r}+\mathbf{u})] + \sum_{s,q=1}^{n/2}\cos 2\pi\mathbf{h}[\mathbf{C}_s\mathbf{r} - \mathbf{C}_q(\mathbf{r}+\mathbf{u})]\Bigg\}\\ &+ 4V^{-2}\sum_{\mathbf{h}\neq\mathbf{k},\mathrm{ind}} m_{c\mathbf{h}}m_{c\mathbf{k}}|F_{\mathbf{h}}F_{\mathbf{k}}|\sum_{s,q=1}^{n/2}\cos[\varphi_p(\mathbf{h})\\ &- 2\pi\mathbf{h}\mathbf{C}_s\mathbf{r}]\cos[\varphi_p(\mathbf{k}) - 2\pi\mathbf{k}\mathbf{C}_q(\mathbf{r}+\mathbf{u})],\end{aligned}$$

then

$$\begin{aligned}\langle\rho(\mathbf{r})\rho(\mathbf{r}+\mathbf{u})\rangle &= \rho_{\mathrm{obs}}(\mathbf{r})\rho_{\mathrm{obs}}(\mathbf{r}+\mathbf{u})\\ &+ 2V^{-2}\sum_{\mathbf{h},\mathrm{ind}}\left|F_{\mathbf{h}}\right|^2(1 - m_{c\mathbf{h}}^2)\\ &\times\sum_{s,q=1}^{n/2}\cos 2\pi\mathbf{h}[\mathbf{C}_s\mathbf{r} - \mathbf{C}_q(\mathbf{r}+\mathbf{u})]\\ &+ 2V^{-2}\sum_{\mathbf{h},\mathrm{ind}}\left|F_{\mathbf{h}}\right|^2(1 - m_{c\mathbf{h}}^2)\\ &\times\sum_{s,q=1}^{n/2}\cos 2\pi\mathbf{h}[\mathbf{C}_s\mathbf{r} + \mathbf{C}_q(\mathbf{r}+\mathbf{u})].\end{aligned}$$

In terms of $\mathbf{r}_A$ and $\mathbf{r}_B$ we obtain

$$\begin{aligned}\langle\rho(\mathbf{r}_A)\rho(\mathbf{r}_B)\rangle &= \rho_{\mathrm{obs}}(\mathbf{r}_A)\rho_{\mathrm{obs}}(\mathbf{r}_B)\\ &+ 2V^{-2}\sum_{\mathbf{h},\mathrm{ind}}\left|F_{\mathbf{h}}\right|^2(1 - m_{c\mathbf{h}}^2)\sum_{s,q=1}^{n/2}\cos 2\pi\mathbf{h}(\mathbf{C}_s\mathbf{r}_A\\ &- \mathbf{C}_q\mathbf{r}_B)\\ &+ 2V^{-2}\sum_{\mathbf{h},\mathrm{ind}}\left|F_{\mathbf{h}}\right|^2(1 - m_{c\mathbf{h}}^2)\sum_{s,q=1}^{n/2}\cos 2\pi\mathbf{h}(\mathbf{C}_s\mathbf{r}_A\\ &+ \mathbf{C}_q\mathbf{r}_B).\end{aligned}\tag{17}$$

If $\mathbf{C}$ belongs to the space-group symmetry operators, $-\mathbf{C}$ also belongs to them. Then equation (17) reduces to

$$\langle\rho(\mathbf{r}_A)\rho(\mathbf{r}_B)\rangle = \rho_{\mathrm{obs}}(\mathbf{r}_A)\rho_{\mathrm{obs}}(\mathbf{r}_B) + T_{\mathrm{c}},$$

where

$$T_{\mathrm{c}} = 2V^{-2}\sum_{\mathbf{h},\mathrm{ind}}\left|F_{\mathbf{h}}\right|^2(1 - m_{c\mathbf{h}}^2)\sum_{s,q=1}^{n}\cos 2\pi\mathbf{h}(\mathbf{C}_s\mathbf{r}_A - \mathbf{C}_q\mathbf{r}_B).\tag{18}$$

If we extend the sum over the $\mathbf{h}$ index to half the measured reciprocal space then the double summation over s and q may be reduced to a simple summation over s; then

$$T_{\mathrm{c}} = V^{-2}\sum_{\mathbf{h}>0}\left|F_{\mathbf{h}}\right|^2(1 - m_{c\mathbf{h}}^2)\sum_{s=1}^{n}\cos[2\pi\mathbf{h}(\mathbf{r}_A - \mathbf{C}_s\mathbf{r}_B)].\tag{19}$$

7. The covariance estimate

Covariance of two random variables x and y is defined by

$$\mathrm{cov}(x, y) = \langle(x - \langle x\rangle)(y - \langle y\rangle)\rangle = \langle xy\rangle - \langle x\rangle\langle y\rangle.$$

It vanishes when x and y are statistically independent. Our study aims to estimate the covariance between the electron densities at two points of a map: in our case $x = \rho(\mathbf{r}_A)$ and $y = \rho(\mathbf{r}_B)$. We can now rewrite equations (14) and (18) in terms of covariance. For non-centrosymmetric space groups we obtain

$$\mathrm{cov}(\mathbf{r}_A, \mathbf{r}_B) = T_{1a} + T_{2a},\tag{20}$$

where T_{1a} and T_{2a} are defined by equations (15*a*), (15*b*) or (16*a*), (16*b*).

For the centrosymmetric case the covariance expression is

$$\mathrm{cov}_{\mathrm{c}}(\mathbf{r}_A, \mathbf{r}_B) = T_{\mathrm{c}},\tag{21}$$

where T_{c} is given by equation (18) or (19).

If $\mathbf{r}_B \equiv \mathbf{r}_A$ or if $\mathbf{r}_B$ is a position symmetry equivalent to $\mathbf{r}_A$, then equations (20) and (21) reduce to the formulas derived by Giacovazzo *et al.* (2011) for estimating the variance in a point of an electron-density map. In particular T_{1a} and T_{2a} reduce to the variance components *TH* and *TD*, respectively, and T_{c} becomes identical to the variance in centric space groups.

To summarize the covariance properties in non-centrosymmetric space groups we notice that the first term of the covariance (say T_{1a}) is related to the Patterson function, the second term (say T_{2a}) to the model. In particular:

(i) T_{1a} is the difference between two terms. The first is the sum of the target Patterson values calculated at the points $(\mathbf{r}_A - \mathbf{C}_s\mathbf{r}_B)$ when s varies over the symmetry operators of the space group. The second is the sum of the weighted target Patterson values, again calculated at the points $(\mathbf{r}_A - \mathbf{C}_s\mathbf{r}_B)$, with model-dependent weights $m_{\mathbf{h}}^2$:

$$T_{1a}(\mathbf{r}_A, \mathbf{r}_B) = V^{-1} \sum_{s=1}^{n} \left[P(\mathbf{r}_A - \mathbf{C}_s\mathbf{r}_B) - P_w(\mathbf{r}_A - \mathbf{C}_s\mathbf{r}_B) \right].$$

When the model is uncorrelated with the target structure

$$T_{1a}(\mathbf{r}_A, \mathbf{r}_B) = V^{-1} \sum_{s=1}^{n} P(\mathbf{r}_A - \mathbf{C}_s\mathbf{r}_B).$$

If the model coincides with the target structure $T_{1a}(\mathbf{r}_A, \mathbf{r}_B) = 0$.

(ii) T_{2a} belongs to the category of observed weighted Fourier synthesis: the phases come from the model, the coefficients (say $|F_{\mathbf{h}}|^2$) from the target, the weights [say $m_{\mathbf{h}}^2 - D_2(X_{\mathbf{h}})$] from the correlation between model and target. Negative minima are expected at the model atomic positions $(\mathbf{r}_A + \mathbf{C}_s\mathbf{r}_B)$.

(iii) Quantitatively, the covariance depends on the correlation between the target and model structures.

In order to illustrate in more detail the relation between covariance and the joint moment $\langle \rho(\mathbf{r}_A)\rho(\mathbf{r}_B) \rangle$, let us suppose that $\mathbf{r}_A$ and $\mathbf{r}_B$ are two atomic positional vectors for both the model and target structures, and that during the phasing process the model is continuously improving (*e.g.*, CORR is continuously increasing). As an effect of the model improvement the joint moment $\langle \rho(\mathbf{r}_A)\rho(\mathbf{r}_B) \rangle$ would increase; that does not imply that $\rho(\mathbf{r}_A)$ and $\rho(\mathbf{r}_B)$ are statistically dependent quantities (they may increase independently of each other, as an effect of the phase variation). To check if $\rho(\mathbf{r}_A)$ and $\rho(\mathbf{r}_B)$ are statistically dependent we should take into consideration $\mathrm{cov}(\mathbf{r}_A, \mathbf{r}_B)$: if it does not vanish, $\rho(\mathbf{r}_A)$ and $\rho(\mathbf{r}_B)$ are statistically dependent. While the variance expression (see Giacovazzo *et al.*, 2011) includes a constant positive term (*i.e.*, the variance is never expected to be negative and oscillates about the constant term), such a term is absent from the covariance formula because covariance may be positive or negative.

In Figs. 1*b*, 2*b* and 3*b* $\mathrm{cov}(z_{\mathrm{O3}}, z_{\mathrm{O3}} + u)$ has been plotted as a black line for the three models. In all three cases a main peak exists: it is a trivial peak, because it corresponds to the covariance between $\rho(z_{\mathrm{O3}})$ and the densities of the pixels belonging to the same z_{O3} peak. Such peak intensity decreases when the model–target correlation decreases. The reason for the existence of the large trivial peak is obvious: the larger the density in z_{O3}, the larger the density in the close pixels.

Close to the main peak there are regions with negative values of the covariance; they correspond to the z_{O3} peak ripples. Also this result is expected; indeed, the larger the density in z_{O3}, the larger and more negative is the density of the ripple pixels.

A third observation is the following: when the model and target structures are very close, then a negative covariance is found between $\rho(z_{\mathrm{O3}})$ and the other two peaks. Indeed, if the phases vary in such a way that the z_{O3} peak increases, the other two peaks should show a smaller intensity to keep the total density unvaried.

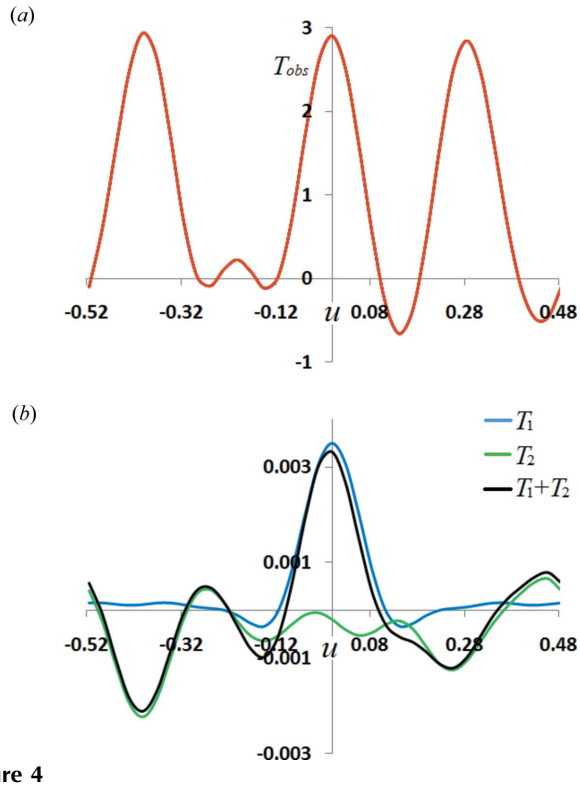

Figure 4
Same model and target structures as for Fig. 1, but with data at 1.8 Å resolution. Components of the $\langle \rho(z_{\mathrm{O3}})(z_{\mathrm{O3}} + u) \rangle$ moment: (*a*) T_{obs} *versus* u; (*b*) T_1 and T_2 *versus* u (in blue and green, respectively). The covariance $(T_1 + T_2)$ is drawn in black.

The analysis of the covariance becomes more complicated in Figs. 2 and 3 where the models significantly differ from the target. Indeed the peak distribution in the $\langle \rho(z_{\mathrm{O3}})\rho(z_{\mathrm{O3}} + u) \rangle$ map (see Figs. 2*a* and 3*a*) simultaneously shows peaks corresponding to interatomic distances present in the target or in the model, plus some additional false peaks. For example, in Fig. 2(*a*) a peak at about $u = -0.40$, corresponding to distance $z_{\mathrm{O1t}} - z_{\mathrm{O3}}$ (z_{O1t} is the z position of O1 in the target structure) and a false peak at about -0.32 are clearly visible. Covariance calculated with respect to $\rho(z_{\mathrm{O3}})$ is negative for the first peak and positive for the second one (the first is suggested from the Patterson, the second from the phases).

Some final general observations on the covariance deserve to be made:

(i) Good models should show small (with respect to T_{obs}) covariances, bad models should suffer with larger covariance values.

(ii) Covariance (in an absolute sense) decreases when data resolution becomes poor. As an example we show in Fig. 4(*a*) $\langle \rho(z_{\mathrm{O3}})\rho(z_{\mathrm{O3}} + u) \rangle$ for the same model used for Fig. 1, calculated by using data up to 1.8 Å resolution. The main features of the covariance are maintained, but in Fig. 4(*b*) covariance is on a smaller scale than in Fig. 1(*b*); the reader will however also notice that $\langle \rho(z_{\mathrm{O3}})\rho(z_{\mathrm{O3}} + u) \rangle$ decreases even more rapidly.

(iii) If data completeness and resolution are both high, if uncertainty of measurement is negligible and phases well assigned, if no structural pseudosymmetry is present, then there is no reason for a substantial covariance in an electron-density map between pairs of points $(\mathbf{r}_A, \mathbf{r}_B)$; in other words, the values of the covariance should be negligible with respect to the corresponding $\langle\rho(\mathbf{r}_A)\rho(\mathbf{r}_B)\rangle$ values. If one or more of the above conditions are violated, a non-negligible covariance should be expected between specific pairs of points in the map; the nature of the pairs would depend on which conditions have been violated. A typical example is the negative covariance between a peak and its ripples, mainly due to data truncation effects rather than to an intrinsic property of the electron-density function. A further example of high covariance is described in Fig. 7 (see below), where the correlation rather than the covariance map is taken into account.

8. Covariance estimate for hybrid electron-density maps

Often one is more interested in the covariance of hybrid rather than of standard electron-density maps; a typical example is the wide use of difference Fourier syntheses, which play an important role not only during the phasing process but also in the later stages of structure refinement. Let us first consider the difference synthesis

$$\rho_q(\mathbf{r}) = \rho(\mathbf{r}) - \rho_p(\mathbf{r}) = 2V^{-1}\sum_{\mathbf{h}>0}|F_{q\mathbf{h}}|\cos(2\pi\mathbf{h}\cdot\mathbf{r} - \varphi_{q\mathbf{h}}),$$

where

$$F_{q\mathbf{h}} = |F_{q\mathbf{h}}|\exp(i\varphi_{q\mathbf{h}}) = |F|\exp(i\varphi_{\mathbf{h}}) - |F_p|\exp(i\varphi_{p\mathbf{h}})$$

is its Fourier coefficient. Then

$$\begin{aligned}\langle\rho_q(\mathbf{r})\rangle &= \langle\rho(\mathbf{r})\rangle - \rho_p(\mathbf{r}) = \rho_{\rm obs}(\mathbf{r}) - \rho_p(\mathbf{r})\\ &= \frac{2}{V}\sum_{\mathbf{h}>0}(m_{\mathbf{h}}|F_{\mathbf{h}}| - |F_{p\mathbf{h}}|)\cos(2\pi\mathbf{h}\cdot\mathbf{r} - \varphi_{q\mathbf{h}})\end{aligned}$$

is its expected value in a point $\mathbf{r}$ [see Main (1979) and Burla *et al.* (2010)]; the mathematical technique described here may also be applied to $\langle\rho_q(\mathbf{r})\rangle$ maps calculated according to Read (1986). If $\rho_q(\mathbf{r}_A) = \rho(\mathbf{r}_A) - \rho_p(\mathbf{r}_A)$ and $\rho_q(\mathbf{r}_B) = \rho(\mathbf{r}_B) - \rho_p(\mathbf{r}_B)$ are the values of the difference electron density at $\mathbf{r}_A$ and $\mathbf{r}_B$, respectively, and if $\langle\rho_q(\mathbf{r}_A)\rho_q(\mathbf{r}_B)\rangle$ and $\mathrm{cov}_q(\mathbf{r}_A, \mathbf{r}_B)$ are the corresponding joint moment and covariance, respectively, then

$$\begin{aligned}\langle\rho_q(\mathbf{r}_A)\rho_q(\mathbf{r}_B)\rangle &= \langle[\rho(\mathbf{r}_A) - \rho_p(\mathbf{r}_A)][\rho(\mathbf{r}_B) - \rho_p(\mathbf{r}_B)]\rangle\\ &= \langle\rho(\mathbf{r}_A)\rho(\mathbf{r}_B)\rangle + \rho_p(\mathbf{r}_A)\rho_p(\mathbf{r}_B)\\ &\quad - \langle\rho(\mathbf{r}_A)\rangle\rho_p(\mathbf{r}_B) - \rho_p(\mathbf{r}_A)\langle\rho(\mathbf{r}_B)\rangle\end{aligned}$$

and

$$\mathrm{cov}_q(\mathbf{r}_A, \mathbf{r}_B) = \mathrm{cov}(\mathbf{r}_A, \mathbf{r}_B).$$

In conclusion, a difference Fourier synthesis shows the same covariance values of the standard electron density.

This result has important effects which may be described by means of the example illustrated in Fig. 5. The target structure is composed of the same three O atoms used for case 1, plus one Li atom at $z_{\rm Li} = 0.314$; the model structure consists of the three O atoms only. At 0.91 Å resolution we calculated a residual between observed and calculated structure factors of 0.23 and we found $\langle\sigma_A\rangle = 0.75$. The observed electron density is shown in Fig. 5(*a*), the difference map calculated *via* coefficients $m_{\mathbf{h}}|F_{\rm obs}| - |F_{\rm calc}|$ (say $\langle\rho_q(\mathbf{r})\rangle$) is shown in Fig. 5(*b*), T_1 and T_2 and the covariance [calculated with respect to $\rho(z_{\rm O3})$] are shown in Fig. 5(*c*). The position of the Li atom is clearly visible in both the observed and the difference electron densities. The covariance shows the usual trivial positive peak, some negative minima corresponding to $\rho(z_{\rm O3})$ ripples and to

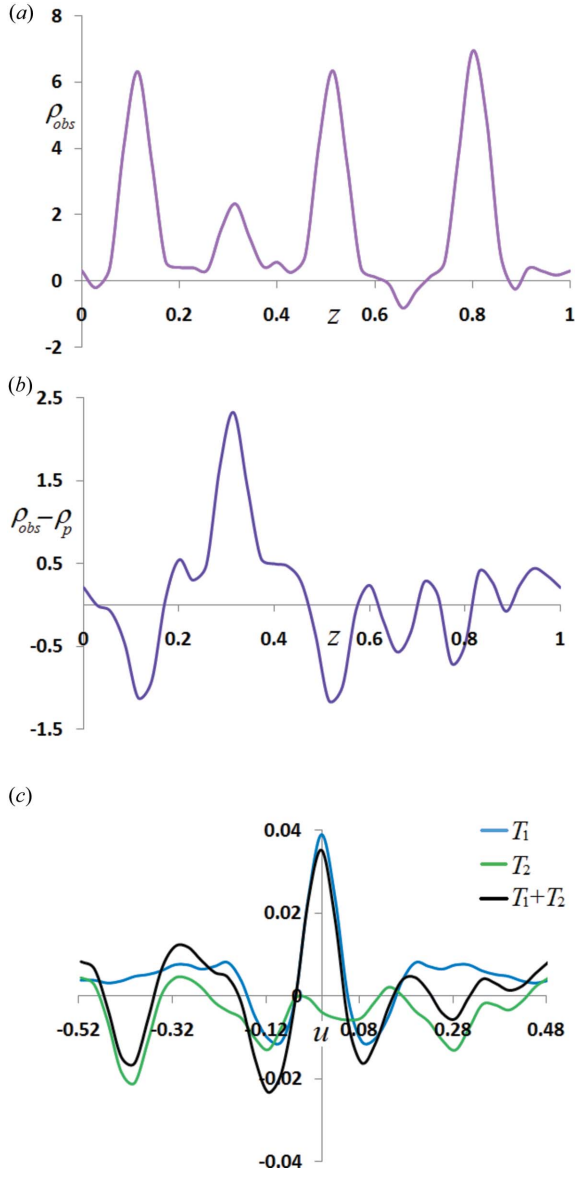

Figure 5
The target structure is composed of the same three O atoms used for Fig. 1 plus one Li atom at $z_{\rm Li} = 0.314$; the model structure consists of the three O atoms only (0.91 Å resolution data). (*a*) Observed electron density; (*b*) difference map calculated *via* coefficients $m_{\mathbf{h}}|F_{\rm obs}| - |F_{\rm calc}|$; components of the $\langle\rho(z_{\rm O3})(z_{\rm O3} + u)\rangle$ moment: (*c*) T_1, T_2 and covariance *versus* u (in blue, green and black, respectively).

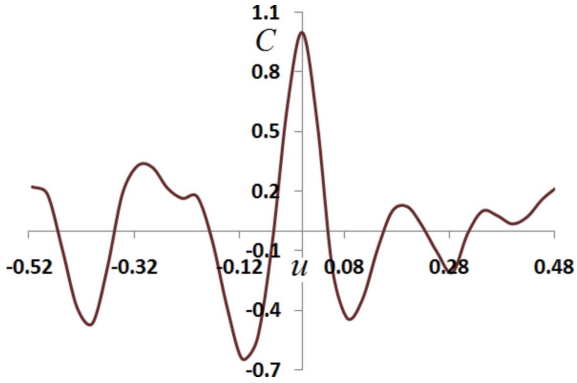

Figure 6
Correlation between the density at z_{O3} and the other density values; target and model structures coincide with those used for Fig. 5.

O1 and O2 positions, and a positive peak in correspondence with the missed Li atom.

Let us now consider the hybrid synthesis

$$\rho_Q(\mathbf{r}) = \tau\rho(\mathbf{r}) - \omega\rho_p(\mathbf{r}) = \frac{2}{V}\sum_{\mathbf{h}>0} |F_Q| \cos(2\pi\mathbf{h}\cdot\mathbf{r} - \varphi_Q).$$

$$F_Q = \tau|F_\mathbf{h}| \exp(i\varphi_\mathbf{h}) - \omega|F_{p\mathbf{h}}| \exp(i\varphi_{p\mathbf{h}})$$

is its Fourier coefficient and

$$\langle\rho_Q(\mathbf{r})\rangle = \frac{2}{V}\sum_{\mathbf{h}>0} (\tau m|F_\mathbf{h}| - \omega|F_{p\mathbf{h}}|) \cos(2\pi\mathbf{h}\cdot\mathbf{r} - \varphi_{p\mathbf{h}})$$

is its expected value. It is easily seen that

$$\mathrm{cov}_Q(\mathbf{r}_A, \mathbf{r}_B) = \tau^2 \mathrm{cov}(\mathbf{r}_A, \mathbf{r}_B). \tag{22}$$

The covariance only depends on the coefficient τ and is insensitive to the value of ω [in agreement with the variance estimates obtained by Giacovazzo *et al.* (2011) for hybrid syntheses].

9. About the correlation estimate

The correlation of two random variables x and y is defined by

$$C(x, y) = \frac{\mathrm{cov}(x, y)}{\sigma_x\sigma_y}, \tag{23}$$

where σ_x and σ_y are the standard deviations of x and y, respectively. While the covariance may take positive or negative values in a range which depends on the standard deviation at the points, the correlation is expected to be in the range $(-1, +1)$. In our notation equation (23) becomes

$$C(\mathbf{r}_A, \mathbf{r}_B) = \frac{\mathrm{cov}(\mathbf{r}_A, \mathbf{r}_B)}{\mathrm{var}^{1/2}[\rho(\mathbf{r}_B)]\mathrm{var}^{1/2}[\rho(\mathbf{r}_B)]},$$

where $\mathrm{var}[\rho(\mathbf{r})]$ is the variance of the map ρ in a point $\mathbf{r}$.

We report for reader usefulness the variance expressions obtained by Giacovazzo *et al.* (2011). In non-centrosymmetric space groups

$$\mathrm{var}\rho(\mathbf{r}) = TH_1 + TH_2(\mathbf{r}) + TD(\mathbf{r}) \tag{24}$$

and

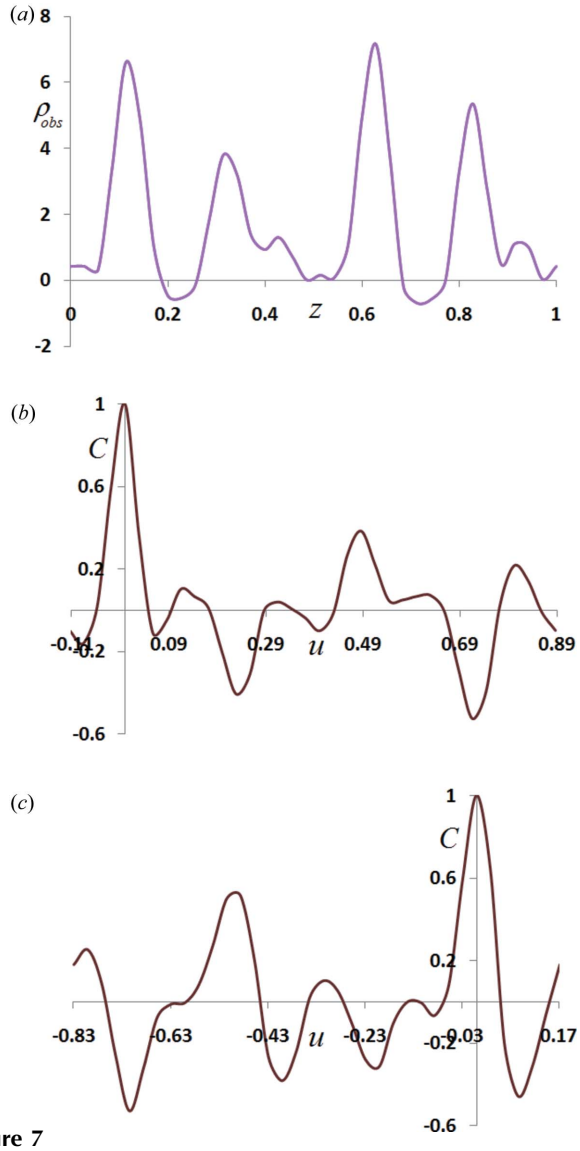

Figure 7
An example of correlation induced by pseudotranslational symmetry (pseudotranslation vector $u_0 = 1/2$). Target structure composed of three O atoms ($z_{O1} = 0.11$, $z_{O2} = 0.63$, $z_{O3} = 0.83$) plus one C atom at $z_C = 0.3$, in the model structure the C atom has been missed, 0.91 Å data resolution. (*a*) Observed electron density; (*b*) correlation map with respect to the density at z_{O1}; (*c*) correlation map with respect to the density at z_{O3}.

$$TH_1 = \frac{2}{V^2}\sum_{\mathbf{h}>0} |F_\mathbf{h}|^2(1 - m_\mathbf{h}^2), \tag{25a}$$

$$TH_2(\mathbf{r}) = \frac{2}{V^2}\sum_{\mathbf{h}>0} |F_\mathbf{h}|^2(1 - m_\mathbf{h}^2)\sum_{s=2}^{n} \cos[2\pi\mathbf{h}(\mathbf{I} - \mathbf{C}_s)\mathbf{r}], \tag{25b}$$

$$TD(\mathbf{r}) = -\frac{2}{V^2}\sum_{\mathbf{h}>0} |F_\mathbf{h}|^2[m_\mathbf{h}^2 - D_2(X_\mathbf{h})]\sum_{s=1}^{n} \cos[2\varphi_p(\mathbf{h}) - 2\pi\mathbf{h}(\mathbf{I} + \mathbf{C}_s)\mathbf{r}]. \tag{25c}$$

In centric space groups

$$\mathrm{var}\rho(\mathbf{r}) = \frac{2}{V^2}\sum_{\mathbf{h}>0} |F_\mathbf{h}|^2(1 - m_{c\mathbf{h}}^2)\sum_{s=1}^{n} \cos[2\pi\mathbf{h}(\mathbf{I} - \mathbf{C}_s)\mathbf{r}]. \tag{26}$$

Let us now consider the correlation coefficient $C_Q(\mathbf{r}_A, \mathbf{r}_B)$ between two points of a hybrid Fourier synthesis. Since $\mathrm{cov}_Q(\mathbf{r}_A, \mathbf{r}_B) = \tau^2 \mathrm{cov}(\mathbf{r}_A, \mathbf{r}_B)$ and $\mathrm{var}_Q^{1/2}[\rho(\mathbf{r})] = \tau \mathrm{var}^{1/2}[\rho(\mathbf{r})]$, it is easily concluded that correlation is insensitive to the type of Fourier synthesis.

To provide the reader with a simple example, we calculated, for the target and model structures depicted in Fig. 5, the correlation between $\rho(z_{O3})$ and the other density values; the result is shown in Fig. 6. Obviously C is equal to 1 for $u = 0$; it regularly decreases until u becomes part of the first ripple, where C becomes negative and attains its absolute minimum (about -0.6). Positive values of C are found in correspondence with the missed Li position and negative values in correspondence with the O1 position.

A further example of non-negligible correlation (and of non-negligible covariance) is shown in Fig. 7; it is generated by the presence of a strong pseudotranslational symmetry. The target structure is composed of three O atoms ($z_{O1} = 0.11$, $z_{O2} = 0.63$, $z_{O3} = 0.83$) and one C atom at $z_C = 0.31$; in the model structure the C atom is missed. We used 0.91 Å resolution data, for which we calculated $\langle \sigma_A \rangle \approx 0.7$. The structure shows a pseudotranslational symmetry with pseudotranslation vector $u_0 = 1/2$ which relates O1 to O2 and O3 to C. In Fig. 7(*a*) the observed electron density is shown: the peak at about 0.31 is a virtuous effect of the observed electron density and of an echo of the O3 peak due to pseudosymmetry (part of the intensity of the O3 peak is transferred to the C peak). In Fig. 7(*b*) the correlation map with respect to the density at z_{O1} is shown; in perfect agreement with expectations, besides the trivial main peak, positive correlation is observed for the peak referred by $u_0 = 1/2$ (say O2) and negative correlation with respect to C and O3 peaks. A similar figure is obtained if the correlation map is calculated with respect to the density at $z_{O2} \approx 0.63$ (not shown for brevity). In Fig. 7(*c*) the correlation map with respect to the density at z_{O3} is shown; the correlation is positive for the C peak, and negative for the O1 and O2 peaks (a similar correlation map is found for the C peak).

10. A general expression of the covariance valid at any stage of the structure analysis

The covariance arising from uncertainty of measurement is negligible when the model is poor, essentially because $\sigma^2(|F_{\mathbf{h}}|)$ is usually quite a small percentage of the $|F_{\mathbf{h}}|^2$ moduli. But even if the model has been refined in a satisfactory way the contribution to the covariance arising from the uncertainty of the phases may still survive, and may be comparable with the contribution coming from the uncertainty of measurement. Indeed it is not rare that some model inadequacy is still present after the refinement; one of the reasons may be the spherical atom assumption, but also inaccurate thermal factor estimates, occupancy factors *etc.* may constitute a supplementary source of covariance. It is therefore useful to combine into a unique expression the contributions arising from phase uncertainties and from uncertainty of measurement.

In §2 we quoted the Rees (1976) expression for the covariance in $P\overline{1}$, valid under the condition that model and target phases coincide. In order to generalize that equation to all acentric space groups, we will consider the electron density

$$\Delta\rho(\mathbf{r}) = \frac{2}{V} \sum_{\mathbf{h},\mathrm{ind}} \Delta|F_{\mathbf{h}}| \sum_{s=1}^{n} \cos[\varphi_p(\mathbf{h}) - 2\pi\mathbf{h}\mathbf{C}_s\mathbf{r}],$$

where $\Delta|F_{\mathbf{h}}| = |F|_{\mathrm{obs}} - |F|_{\mathrm{true}}$. The following reasonable assumptions will hold:

(i) the same $\Delta|F|$ is associated to symmetry-equivalent reflections;

(ii) $\langle \Delta|F| \rangle = 0$ and $\langle \Delta|F_{\mathbf{h}}| \Delta|F_{\mathbf{k}}| \rangle = 0$ if $\mathbf{h} \neq \mathbf{k}$;

(iii) $\langle \Delta|F_{\mathbf{h}}| \Delta|F_{\mathbf{h}}| \rangle = \sigma^2(|F_{\mathbf{h}}|)$, where $\sigma(|F_{\mathbf{h}}|)$ is the standard deviation of the observed structure-factor modulus.

Under the above assumptions the corresponding contribution to the covariance is

$$\begin{aligned}\Delta\mathrm{cov}(\mathbf{r}_A, \mathbf{r}_B) = {} & \frac{2}{V^2} \sum_{\mathbf{h}>0} \sigma^2(|F_{\mathbf{h}}|) \sum_{s=1}^{n} \cos[2\pi\mathbf{h}(\mathbf{r}_A - \mathbf{C}_s\mathbf{r}_B)] \\ & + \frac{2}{V^2} \sum_{\mathbf{h}>0} \sigma^2(|F_{\mathbf{h}}|) \sum_{s=1}^{n} \cos[2\varphi_p(\mathbf{h}) \\ & - 2\pi\mathbf{h}(\mathbf{r}_A + \mathbf{C}_s\mathbf{r}_B)]. \end{aligned} \tag{27}$$

If we suppose that the uncertainty of measurement (depending on the experiment) is statistically independent of the phase uncertainty (which depends on the model) we can combine equation (27) with equation (20) to obtain a general expression valid at any stage of the crystallographic phasing:

$$\mathrm{cov}(\mathbf{r}_A, \mathbf{r}_B) = T_{a1t} + T_{a2t}, \tag{28}$$

where

$$\begin{aligned} T_{a1t} = {} & \frac{2}{V^2} \sum_{\mathbf{h}>0} \left[\sigma^2(|F_{\mathbf{h}}|) + |F_{\mathbf{h}}|^2(1 - m_{\mathbf{h}}^2)\right] \\ & \times \sum_{s=1}^{n} \cos[2\pi\mathbf{h}(\mathbf{r}_A - \mathbf{C}_s\mathbf{r}_B)] \end{aligned} \tag{29a}$$

$$\begin{aligned} T_{a2t} = {} & -\frac{2}{V^2} \sum_{\mathbf{h}>0} \left\{|F_{\mathbf{h}}|^2[m_{\mathbf{h}}^2 - D_2(X_{\mathbf{h}})] - \sigma^2(|F_{\mathbf{h}}|)\right\} \\ & \times \sum_{s=1}^{n} \cos[2\varphi_p(\mathbf{h}) - 2\pi\mathbf{h}(\mathbf{r}_A + \mathbf{C}_s\mathbf{r}_B)]. \end{aligned} \tag{29b}$$

For centrosymmetric space groups the combined formula [see equation (21)] is

$$\mathrm{cov}_c(\mathbf{r}_A, \mathbf{r}_B) = T_{c2}, \tag{30}$$

where

$$\begin{aligned} T_{c2} = {} & \frac{2}{V^2} \sum_{\mathbf{h}>0} \left[\sigma^2(|F_{\mathbf{h}}|) + |F_{\mathbf{h}}|^2(1 - m_{c\mathbf{h}}^2)\right] \\ & \times \sum_{s=1}^{n} \cos[2\pi\mathbf{h}(\mathbf{r}_A - \mathbf{C}_s\mathbf{r}_B)]. \end{aligned} \tag{31}$$

When $\mathbf{r}_A = \mathbf{C}_s\mathbf{r}_B$ the covariance expressions (28), (29*a*), (29*b*), (30), (31) coincide with the equations derived by Giacovazzo *et al.* (2011) for the variance.

11. Conclusions

Covariance between two points of an electron-density map has seldom been the object of study (Rees, 1976, 1978) even if it deals with fundamental aspects of the Fourier syntheses. A general theory has been described here which provides covariance estimates at any stage of the phasing process (*i.e.* for any model quality) and for any centrosymmetric or non-centrosymmetric space group. It has been shown that, of the two terms contributing to the variance estimate, one is related to the Patterson function, the other to the model. The covariance between two points varies with the correlation between target and model structure, is space-group dependent and varies with data resolution. A formal expression of the correlation between the electron densities of two points of any type of Fourier map has been given. A general formula has been derived which also takes into account the uncertainty on the diffraction moduli. The theory has been generalized to any type of hybrid Fourier synthesis.

APPENDIX *A*

To demonstrate that equations (15*a*) and (16*a*) are identical, we apply the symmetry operator algebra as follows [see *International Tables for Crystallography* (Wondratschek, 1992)]:

$$\begin{aligned}2\pi\mathbf{h}(\mathbf{C}_s\mathbf{r}_A-\mathbf{C}_q\mathbf{r}_B)&=2\pi\mathbf{h}\mathbf{R}_s(\mathbf{r}_A-\mathbf{R}_s^{-1}\mathbf{R}_q\mathbf{r}_B)+2\pi\mathbf{h}(\mathbf{T}_s-\mathbf{T}_q)\\&=2\pi\mathbf{h}\mathbf{R}_s(\mathbf{r}_A-\mathbf{R}_\tau\mathbf{r}_B)+2\pi\mathbf{h}(\mathbf{T}_s-\mathbf{T}_q),\end{aligned}\tag{32}$$

where $\mathbf{C}_\tau=\mathbf{C}_s^{-1}\mathbf{C}_q$ and

$$\mathbf{R}_\tau=\mathbf{R}_s^{-1}\mathbf{R}_q,\qquad \mathbf{T}_\tau=\mathbf{R}_s^{-1}\mathbf{T}_q+\mathbf{T}_s^{-1}.\tag{33}$$

Since

$$\mathbf{T}_s^{-1}=-\mathbf{R}_s^{-1}\mathbf{T}_s\tag{34}$$

we have

$$2\pi\mathbf{h}(\mathbf{T}_s-\mathbf{T}_q)=2\pi\mathbf{h}\mathbf{R}_s(\mathbf{R}_s^{-1}\mathbf{T}_s-\mathbf{R}_s^{-1}\mathbf{T}_q)=-2\pi\mathbf{h}\mathbf{R}_s\mathbf{T}_\tau.\tag{35}$$

Combining equations (35) and (32) gives

$$2\pi\mathbf{h}(\mathbf{C}_s\mathbf{r}_A-\mathbf{C}_q\mathbf{r}_B)=2\pi\mathbf{h}\mathbf{R}_s(\mathbf{r}_A-\mathbf{C}_\tau\mathbf{r}_B),$$

which makes equations (15*a*) and (16*a*) identical.

The above results may easily demonstrate that equations (15*b*) and (16*b*) are identical. Indeed

$$\begin{aligned}2\varphi_{\mathbf{h}}-2\pi\mathbf{h}(\mathbf{C}_s\mathbf{r}_A+\mathbf{C}_q\mathbf{r}_B)&=2\varphi_{\mathbf{h}\mathbf{R}s}+4\pi\mathbf{h}\mathbf{T}_s-2\pi\mathbf{h}\mathbf{R}_s(\mathbf{r}_A+\mathbf{R}_\tau\mathbf{r}_B)\\&\quad-2\pi\mathbf{h}(\mathbf{T}_s+\mathbf{T}_q)\\&=2\varphi_{\mathbf{h}\mathbf{R}s}-2\pi\mathbf{h}\mathbf{R}_s(\mathbf{r}_A+\mathbf{R}_\tau\mathbf{r}_B)\\&\quad+2\pi\mathbf{h}(\mathbf{T}_s-\mathbf{T}_q).\end{aligned}$$

In accordance with equation (35) we have

$$2\varphi_{\mathbf{h}}-2\pi\mathbf{h}(\mathbf{C}_s\mathbf{r}_A+\mathbf{C}_q\mathbf{r}_B)=2\varphi_{\mathbf{h}\mathbf{R}s}-2\pi\mathbf{h}\mathbf{R}_s(\mathbf{r}_A+\mathbf{C}_\tau\mathbf{r}_B).$$

References

Booth, A. D. (1946). *Proc. R. Soc. London Ser. A*, **188**, 77–92.
Booth, A. D. (1947). *Proc. R. Soc. London Ser. A*, **190**, 482–489.
Bragg, W. L. & West, J. (1930). *Philos. Mag.* **10**, 823–824.
Burla, M. C., Caliandro, R., Carrozzini, B., Cascarano, G. L., De Caro, L., Giacovazzo, C., Polidori, G. & Siliqi, D. (2006). *J. Appl. Cryst.* **39**, 527–535.
Burla, M. C., Caliandro, R., Giacovazzo, C. & Polidori, G. (2010). *Acta Cryst.* A**66**, 347–361.
Burla, M. C., Giacovazzo, C., Mazzone, A., Polidori, G. & Siliqi, D. (2011). *Acta Cryst.* A**67**, 276–283.
Caliandro, R., Carrozzini, B., Cascarano, G. L., De Caro, L., Giacovazzo, C. & Siliqi, D. (2007). *J. Appl. Cryst.* **40**, 883–890.
Cochran, W. (1951). *Acta Cryst.* **4**, 408–411.
Cruickshank, D. W. J. (1949). *Acta Cryst.* **2**, 65–82.
Cruickshank, D. W. J. & Rollett, J. S. (1953). *Acta Cryst.* **6**, 705–707.
Giacovazzo, C. & Mazzone, A. (2011). *Acta Cryst.* A**67**, 210–218.
Giacovazzo, C., Mazzone, A. & Comunale, G. (2011). *Acta Cryst.* A**67**, 368–382.
Main, P. (1979). *Acta Cryst.* A**35**, 779–785.
Mises, R. von (1918). *Z. Phys.* **19**, 490–500.
Read, R. J. (1986). *Acta Cryst.* A**42**, 140–149.
Rees, B. (1976). *Acta Cryst.* A**32**, 483–488.
Rees, B. (1978). *Acta Cryst.* A**34**, 254–256.
Sim, G. A. (1959). *Acta Cryst.* **12**, 813–815.
Srinivasan, R. & Ramachandran, G. N. (1965). *Acta Cryst.* **19**, 1008–1014.
Wondratschek, H. (1992). *International Tables for Crystallography*, Vol. A, pp. 709–748. Dordrecht, Boston: Kluwer Academic Publishers.